A B–spline based higher order method in 3D.

H. Maniar
MIT, Cambridge, MA 02139, USA

In wave–body interactions, to capture the variability of the potential accurately, low order panel methods often require a fine discretization of the body. Consequently, the computational effort required to set–up and solve the system of equations is increased. In an effort to alleviate this problem, higher order panel methods have been proposed in the past. Besides achieving better accuracy for coarser discretizations, obtaining tangential derivatives in a higher order method requires little additional effort and is numerically more robust.

We present here a new higher order panel method, where both the potential and geometry are B–spline tensor product expansions, and apply it to the linear analysis of radiation/diffraction problems in three dimensions. An earlier B–spline based approach in two dimensions for exterior infinite fluid flows was reported in [1]. In the following we briefly outline the scheme and then present results which validate and help evaluate its performance.

1. <u>Outline of the scheme</u> Let the wetted portion of the body be composed of several large curvilinear patches. By 'large' we imply that some characteristic length scale of the patch can be of the same order of magnitude as that of the body. Each patch is a parameterised surface with its Cartesian components given by a B–spline tensor product expansion (as contructed by some geometric modelling package). In practice, these expansions can describe a body very accurately.

On the parametric space of each patch the solution surface is modelled by proposing the potential as a B–spline tensor product expansion, whose unknown complex coefficients are to be solved for (henceforth, B–splines are understood to mean B–spline tensor products). The B–splines as used in the geometry and potential representations are not necessarily the same, since their orders and the knot vectors they are built on can be different. Implicit in the potential representation is the fact that an expansion based on kth–order B–splines has $(k-2)$ degrees of continuity ensured everywhere on the patch. Hence, with an appropriately chosen order, even higher derivatives of the potential retain some degree of continuity everywhere on the patch. For bodies composed of several patches, no explicit conditions are imposed on the potentials at/or across the common boundaries of patches.

Denoting the approximate potential and normal derivative on the body by ϕ and $\partial\phi/\partial n$ and using Green's theorem, we define the residual, $\tilde{r}$, for radiation problems as,

$$\tilde{r} = 2\pi\phi + \iint_{\Gamma} \phi \frac{\partial G}{\partial n}\, dS - \iint_{\Gamma} \frac{\partial \phi}{\partial n} G \, dS$$

and for diffraction problems, the last term is to be replaced by $-4\pi\phi_I$, the incident wave potential. Above, G is the Green function which satisfies all the linearized boundary conditions except that on the body. Further, for radiation problems the normal derivative is approximated by local Taylor expansions in parametric variables between consecutive non–coincident knots.

A Galerkin procedure is employed to obtain a complex system of equations for the unknown complex coefficients of the potential B–spline expansion. Specifically, we minimize the residual with respect to the each of the (potential) B–splines directly over the parametric space of their support. Since the potential B–spline expansion over every patch is a sum of products of an unknown coefficient and a B–spline, we have exactly as many B–splines to minimize the residual with as unknowns. Thus, every patch provides exactly the same number of equations as the unknowns over that patch, resulting in a square complex dense system of equations.

The matrix entries require evaluating double spatial integrals due to the Galerkin step. They are evaluated semi–discretely, where the outer integrals are evaluated by a fixed order product Gauss rule and the inner evaluated exactly (i.e., accurately). In practice, the outer integral is further subdivided onto those over the space between consecutive knots of the B–spline the residual is being minimized with and a product Gauss–Legendre rule applied to each. Thus the Cartesian coordinates of the Gauss nodes of the outer integrals provide the field points for the inner integrals. One is then required to evaluate influence coefficients and their moments over curved surfaces. Special algorithms have been developed for handling the Rankine singularities over curved surfaces. The near field is evaluated by an adaptive subdivision scheme, while in the self–influence case, the singularities are analytically removed and the desingularised integrands are expanded in a series with algebraic type terms which are integrable. A product Gauss–Legendre rule is used to evaluate the free–surface part of the Green function over curved surfaces, with the functional evaluations by special algorithms described in [4].

2. **Results** Analytic or benchmark results exist for the added mass/damping of a floating unit hemisphere [2], the exciting force on a submerged spheroid [3] and the potential on a bottom–mounted circular cylinder [5]. We compare these results with our computations. In each case the bodies are represented by B–spline expansions which are practically exact. The degree of the potential B–splines for all the cases is cubic and for radiation problems, the normal derivative expansions are truncated homogeneously at degree 4. The outer integration is a fixed 3×3 product Gauss–Legendre rule. 'Panels' are defined as the space between consecutive non–coincident knots. To minimize round–off contributions to errors due to approximations in the scheme, all computations were performed in double precision. All the errors quoted are absolute.

Making use of the symmetry, a quadrant of a floating unit hemisphere ($a = 1$) is modelled as a patch. Comparing the heave/surge added mass and damping with the tabulated results in [2], for $ka \leq 1$, agreement to all four decimals is achieved with 3×3 panels/quad. (6×6 unknowns/quad.). For $6 \geq ka > 1$, 4×4 panels/quad. (7×7 unknowns/quad.) results in an error of 0.01%. Fig. 1(i) compares the heave added mass/damping with results from [2]; with the above mentioned accuracy the different discretizations are indistinguishable. The scheme is not immune to the effects of irregular frequencies, but unlike constant panel methods, the bandwidth is very limited even for low discretizations. Fig. 1(ii) displays more accurately the bandwidth reduction of the polluted region with increasingly accurate solutions through finer discretizations. Similar results have been observed for a hemisphere in surge and a truncated floating circular cylinder in heave and surge.

Tables 2(i),(ii) are the absolute errors in the real and imaginary vertical exciting force (normalized) on a submerged spheroid in head seas [3]. The ratio of major to minor axis is $a : b = 6 : 1$, and the depth of submergence of its center is $2b$. Symmetry is made use of and the 'panels'/unknowns indicated are per quadrant of the spheroid. The accuracy of the scheme is self–evident.

Numerically, the diffraction force on a bottom mounted circular cylinder is relatively easy to obtain compared to the potential itself for short incident waves, since only the first angular mode contributes to the force while several modes contribute significantly to the potential. For $1 \le ka \le 8$ at least 7–19 angular modes need to be retained in the analytic potential expansion for a 5D accuracy and perhaps reflects the difficulty of the short wave solution. For a cylinder of unit radius ($a = 1$) and depth $= 1/2$, we tabulate in 3(i)–(iv), the normalised (igA/ω) run–up due to incident waves, $ka = 1, 2, 4, 8$ respectively at a few select angles. The left half of each table compares the real part of the run–up for various discretizations, and the right half the imaginary part. The 'panels' and unknowns indicated are per half–body of the cylinder. The rapid convergence evident for long waves seems to slow down for short waves. Nevertheless, accurate pointwise values are still possible with practical discretizations.

This work was supported by the Joint Industry Project 'Wave effects on offshore structures'.

References

[1] Hsin, C.–Y., Kerwin, J.E. and Newman, J.N., "A higher order panel method based on B–splines", Sixth International Conference on Numerical Ship Hydrodynamics, Iowa City, Iowa, 2 August 1993.

[2] Hulme, A., "The wave forces acting on a floating hemisphere undergoing forced periodic oscillations.", J. Fluid Mech., vol.121, pp. 443–463, 1982.

[3] Wu, G.X. and Eatock Taylor, R., "The exciting forces on a submerged spheroid in regular waves.", J. Fluid Mech., vol.182, pp. 411–426, 1987.

[4] Newman, J.N, "The approximation of free–surface Green functions", in 'Wave Asymptotics', P.A. Martin & G.R. Wickham, editors, Cambridge University Press, 1992.

[5] Mei, C.C, "The Applied Dynamics of Ocean surface waves", World Scientific Publishing Co. Pte. Ltd., 1989.

Figure 1(i): Hemisphere in heave

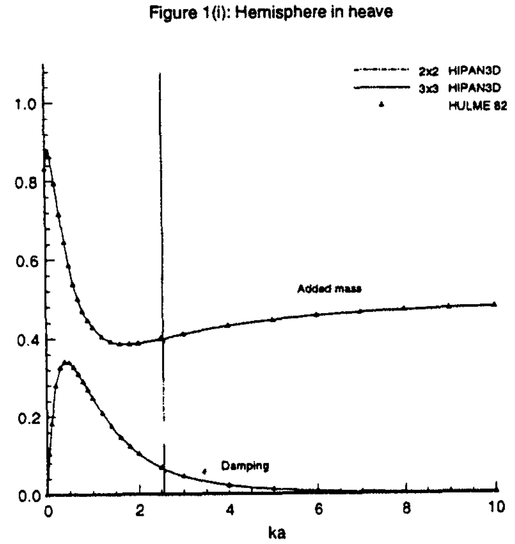

Figure 1(ii): 'Irregular frequency' bandwidth for heaving hemisphere

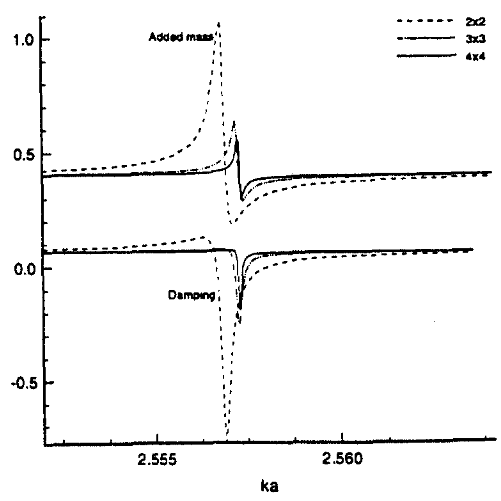

Tables 2(i),(ii): **Vertical exciting force on a submerged spheroid in head seas.**

ka	Wu & E.–Taylor	Absolute Error			
		2x2 *panels*	3x3 *panels*	4x4 *panels*	5x5 *panels*
		5x5 *unkn.'s*	6x6 *unkn.'s*	7x7 *unkn.'s*	8x8 *unkn.'s*
0.1	2.0256	0.0003	0.0001	0.0000	0.0000
0.4	2.0466	0.0002	0.0001	0.0000	0.0000
1.0	1.9871	0.0000	0.0000	0.0000	0.0000
4.0	0.0453	0.0045	0.0006	0.0007	0.0006
5.0	-0.1904	0.0120	0.0002	0.0000	0.0001

ka	Wu & E.–Taylor	Absolute Error			
		2x2 *panels*	3x3 *panels*	4x4 *panels*	5x5 *panels*
		5x5 *unkn.'s*	6x6 *unkn.'s*	7x7 *unkn.'s*	8x8 *unkn.'s*
0.1	0.0002	0.0000	0.0000	0.0000	0.0000
0.4	0.0121	0.0000	0.0000	0.0000	0.0000
1.0	0.1265	0.0000	0.0000	0.0000	0.0000
4.0	0.1397	0.0034	0.0005	0.0005	0.0005
5.0	0.0139	0.0048	0.0001	0.0000	0.0000

Tables 3(i)-(iv): **Run–up on a bottom mounted circular cylinder: ka = 1,2,4,8**

θ	Exact *Re*	Absolute Error			Exact *Im*	Absolute Error		
		6x1 *panels*	12x2 *panels*	24x4 *panels*		6x1 *panels*	12x2 *panels*	24x4 *panels*
		9x4 *unkn's*	15x5 *unkn's*	27x7 *unkn's*		9x4 *unkn's*	15x5 *unkn's*	27x7 *unkn's*
0	0.60696	0.66754	0.00002	0.00000	-1.59553	0.48192	0.00002	0.00000
45	0.94854	0.20103	0.00004	0.00001	-1.31312	0.05436	0.00001	0.00000
90	1.13044	-0.21267	0.00005	0.00000	-0.30661	0.15922	0.00001	0.00000
135	0.26870	0.00069	0.00003	0.00000	0.61619	0.19736	0.00003	0.00000
180	-0.35334	0.36767	0.00002	0.00000	0.81489	1.15585	0.00003	0.00000

θ	Exact *Re*	Absolute Error			Exact *Im*	Absolute Error		
		6x1 *panels*	12x2 *panels*	24x4 *panels*		6x1 *panels*	12x2 *panels*	24x4 *panels*
		9x4 *unkn's*	15x5 *unkn's*	27x7 *unkn's*		9x4 *unkn's*	15x5 *unkn's*	27x7 *unkn's*
0	-1.02073	2.08989	0.00003	0.00000	-1.55315	5.49009	0.00008	0.00001
45	-0.07468	0.49727	0.00026	0.00001	-1.71268	0.20280	0.00016	0.00002
90	1.29456	0.22064	0.00029	0.00001	-0.07267	0.19733	0.00006	0.00000
135	-0.01615	0.12901	0.00035	0.00002	0.64158	0.29323	0.00002	0.00000
180	-0.59385	0.55099	0.00008	0.00001	-0.42772	1.52793	0.00017	0.00001

θ	Exact *Re*	Absolute Error			Exact *Im*	Absolute Error		
		6x1 *panels*	12x2 *panels*	24x4 *panels*		6x1 *panels*	12x2 *panels*	24x4 *panels*
		9x4 *unkn's*	15x5 *unkn's*	27x7 *unkn's*		9x4 *unkn's*	15x5 *unkn's*	27x7 *unkn's*
0	-1.11917	3.94924	0.00171	0.00006	1.59278	1.18575	0.00167	0.00005
45	-1.77564	0.18028	0.00162	0.00009	-0.34243	0.52946	0.00307	0.00014
90	1.31949	0.02861	0.00414	0.00014	-0.06133	0.05094	0.00105	0.00005
135	-0.64824	0.03664	0.00095	0.00003	-0.34343	0.27795	0.00378	0.00016
180	0.34643	0.40560	0.00092	0.00001	0.41848	1.14534	0.00240	0.00011

θ	Exact *Re*	Absolute Error			Exact *Im*	Absolute Error		
		6x1 *panels*	12x2 *panels*	24x4 *panels*		6x1 *panels*	12x2 *panels*	24x4 *panels*
		9x4 *unkn's*	15x5 *unkn's*	27x7 *unkn's*		9x4 *unkn's*	15x5 *unkn's*	27x7 *unkn's*
0	-0.40422	7.60443	0.01768	0.00037	-1.93885	2.38158	0.03155	0.00195
45	1.62434	0.17415	0.03144	0.00050	0.96750	3.39658	0.04162	0.00160
90	1.34517	0.69713	0.08058	0.00268	-0.05335	0.66881	0.02175	0.00079
135	0.46963	0.12650	0.03086	0.00002	0.34171	0.59344	0.06261	0.00169
180	0.13773	0.96278	0.05209	0.00035	0.33188	4.12517	0.05409	0.00123

DISCUSSION

Yue, D. K. P.,: You showed a result showing asymptotic (large *N*) convergence rate of $O(N^{-1})$ which seems much too slow for cubic spline representations. What would you expect the convergence rate to be for your method?

Maniar, H.: I am not aware of theoretical convergence rates for this scheme. Only recently has the validation step of the scheme been completed and now we are addressing issues like convergence rates. So far, to estimate, with some confidence, convergence rates through numerical experimentation and comparison with exact/benchmark results has been difficult. This is mainly because, either the scheme is very accurate with a few panels (e.g. diffraction force on a bottom mounted circular cylinder) and/or benchmark results are available to an insufficient number of significant digits to infer a meaningful convergence rate (cf. the table for diffraction forces on a submerged spheroid).

Nevertheless, the added mass of a translating sphere in an infinite fluid and the horizontal mean drift forces on a bottom mounted circular cylinder seem to provide an opportunity. If *N*=total number of unknowns, and we expect an error proportional to *(1/N)**p*, then in the former case we have p=3 for a linear potential and p=6 for a quadratic potential.

The results shown at the workshop were for the horizontal mean drift force on a bottom mounted circular cylinder. Convergence rates for the total force and the water line integral contribution (the surface integral contribution is similar) were shown. For a cubic potential approximation, the total force converged rapidly, but the water line integral contribution converged at a relatively slower rate (reduced to linear convergence for large *N*). Since then, we have re-examined the specific problem and attribute the relatively slow convergence rate to outer Gauss integration error (residual minimization step). A new computation with more accurate outer integration shows the water line integral to converge cubically (p=3).

Martin, P. A.: You are using B-splines for both the unknown potential and the surface geometry. As I understand the situation, many CAD systems represent surfaces using so-called *Non-uniform Rational B-Splines* (NURBS); these are just the ratio of two splines. Have you tried doing this? It has been tried recently in a different context by Valle *et al.* (1).

Note: It would be hopeless to use NURBS to represent the unknown potential, because this would lead to a *nonlinear* algebraic system (for the unknown coefficients in the denominators of the NURBS).

(1) Valle, L., Rivas, F. & Cátedra, M. F. (1994) Combining the moment method with geometrical modelling by NURBS surfaces and Bézier patches. *IEEE Trans.* ***AP-42***, 373-381,

Maniar, H.: No, I have not tried using NURBS surface representations in the scheme. But, in the early development of the scheme I did give it a brief thought. Since the current scheme utilizes surface polynomials (in the parametric space) for the self-influence algorithm and the normal derivative of the potential, rational polynomials (NURBS) were ruled out.

Yeung, R. W.: Scott Coackley of my department has recently completed a Bi-cubic Surface Spline method for wave and body interaction, though for a different problem. I am pleased to see that the types of convergence and accuracy reported in your abstract are consistent with our favourable experience. I have two questions. The first is that it seems sufficient to use a collocation method instead of a Galerkin form for the integral equation. I am curious why the latter is chosen. Second, we experience some difficulties with mapping the pointed end of the body (say the poles of a sphere) to the spline (u-v) parametric space. This is a singular point in the mapping and the geometric difficulties lead to higher errors in the solution at these points. I wonder if you have a better way of circumventing this problem.

Maniar, H.: In general, the number of unknowns (coefficients of the potential B-spline expansions) and the number of 'panels' are not equal. If no conditions are imposed on the potential, one must pick as many collocation points as unknowns, and this would require selecting points besides, say, the centroid. Practically, for an arbitrary body, this would be difficult and non-robust. Alternatively, presumably the total number of unknowns may be reduced by imposing some conditions on the potential. For complex bodies or bodies with corners, to impose conditions other than functional continuity across patches (in a compositely built body), would require anticipating the solution and may be difficult. We consider the Galerkin approach a robust alternative.

Mapping a 'topologically' triangular surface to a rectangular parametric space will introduce a singularity (vanishing Jacobian) at some point. Currently, we use a least squares fitting procedure to model the geometry and, at times, have encountered some difficulty due to this singular mapping. But, with the introduction of 'sufficient' additional B-splines to aid the fit, the least squares procedure seems to reduce the error (deviation from the exact surface) and 'localize' it to the region near the singular parameterization.

For bodies with singular mapping, the only results I have obtained have been integrated quantities. In general, these results are fairly accurate and the presence of this singular point must not affect the solution globally. Substantial error, if any, introduced due to the singular mapping must be local.